Clinical implications of organ congestion in heart failure patients as assessed by ultrasonography

Yoshihiro Seo[1], Tomofumi Nakatsukasa[2], Seika Sai[2], Tomoko Ishizu[1,3], Noriko Iida[4], Masayoshi Yamamoto[1], Tomoko Machino-Ohtsuka[1], Yasushi Kawakami[3], Akihiko Nogami[1], Kazutaka Aonuma[1]

[1]Department of Cardiology, Faculty of Medicine, [2]Department of Cardiology, Graduate School of Comprehensive Human Sciences, [3]Department of Clinical Laboratory Medicine, Faculty of Medicine, University of Tsukuba, Tsukuba, Japan; [4]Clinical Laboratory, University of Tsukuba Hospital, Tsukuba, Japan

Contributions: (I) Conception and design: Y Seo, K Aonuma, Y Kawakami, A Nogami; (II) Administrative support: None; (III) Provision of study materials or patients: All authors; (IV) Collection and assembly of data: T Nakatsukasa, S Sai, T Ishizu, N Iida, M Yamamoto; (V) Data analysis and interpretation: Y Seo, T Nakatsukasa, S Sai, T Ishizu, N Iida; (VI) Manuscript writing: All authors; (VII) Final approval of manuscript: All authors.

Correspondence to: Yoshihiro Seo, MD. Cardiovascular Division, Faculty of Medicine, University of Tsukuba, 1-1-1 Tennodai, Tsukuba 305-8575, Japan. Email: yo-seo@md.tsukuba.ac.jp.

Abstract: In the management of heart failure (HF), decongestion is critical for improving clinical outcomes in addition to patients' symptoms. Although physicians accept this theory, there are no established markers for the achievement of optimal decongestion status. Organ congestion, in particular liver and kidney congestion, has recently attracted substantial attention. Ultrasound methods have been introduced for assessing organ congestion, although this is merely a preliminary step. Here, we review the clinical implications of the assessment of organ congestion by ultrasound.

Keywords: Decongestion; Doppler ultrasonography; heart failure (HF); organ congestion

Introduction

Heart failure (HF) is a current epidemic of cardiovascular disease (1). Despite several evidence-based medical therapies, patients with HF experience repeated hospitalization and have poor prognosis (2). In addition, HF-related medical costs are increasingly straining economies worldwide (3). In clinical settings, physical signs, chest X-ray, electrocardiogram, and biomarkers including natriuretic peptides are used to diagnosis HF among patients with dyspnea (*Table 1*) (4). In contrast, these findings are adopted for the management of HF patients, since it is important to maintain a stable condition, which requires optimal decongestion status (5). In addition, Doppler echocardiography has a central role in the assessment of the functional and hemodynamic status of HF patients (6). Despite such comprehensive evaluations of the decongestion status in HF patients, the prognosis of HF remains poor (5).

Organ congestion in HF patients has recently attracted attention as a novel therapeutic guide to achieve optimal decongestion instead of central venous pressure (CVP). Accordingly, in this review, we describe the ultrasonography-based assessment of organ congestion and clinical implications for the management of HF patients.

Liver stiffness (LS) related to congestion in cardiac-hepatopathy

Hepatic injury related to cardiac disease, termed "cardiac hepatopathy", is common (7). The major manifestation is passive congestive hepatopathy, which was first described by Dr. Sheila Sherlock in 1951; passive congestive hepatopathy is caused by right-sided HF including biventricular HF, pulmonary artery hypertension, significant tricuspid regurgitation, constrictive pericarditis, and congenital heart

58

Seo et al. Assessment of organ congestion by ultrasonography

Table 1 Summary of diagnostic accuracy for heart failure in emergency outpatients

Findings	Sensitivity (%)	Specificity (%)	Positive LR (95% CI)	Negative LR (95% CI)
Physical examination				
S3 gallop	13	99	11 (4.9–25)	0.88 (0.83–0.94)
Abdominojugular reflux	24	96	6.4 (0.81–51)	0.79 (0.62–1.0)
JVD	39	92	5.1 (3.2–7.9)	0.66 (0.57–0.77)
Crackles	60	78	2.8 (1.9–4.1)	0.51 (0.37–0.70)
Heart murmur	27	90	2.6 (1.7–4.1)	0.81 (0.73–0.90)
Leg edema	50	78	2.3 (1.5–3.7)	0.64 (0.47–0.87)
Wheeze	22	58	0.52 (0.38–0.71)	1.3 (1.1–1.7)
Chest X-ray				
Lung edema	54	96	12 (6.8–21)	0.48 (0.28–0.83)
Interstitial edema	34	97	12 (5.2–27)	0.68 (0.54–0.85)
Cardiomegaly	74	78	3.3 (2.4–4.7)	0.33 (0.23–0.43)
Electrocardiogram				
Atrial fibrillation	26	93	3.8 (1.7–8.8)	0.79 (0.65–0.96)
Any abnormal finings	50	78	2.2 (1.6–3.1)	0.64 (0.47–0.88)
Laboratory data				
BNP >100 pg/mL	93	66	2.7 (2.0–3.9)	0.11 (0.07–0.16)

Quoted from reference (4). BNP, B-type natriuretic peptide; LR, likelihood ratio; JVD, jugular vein distention.

diseases (8). The hemodynamic determinant of congestive hepatopathy is increased CVP, i.e., the higher filling pressure required to counteract increased right ventricular diastolic pressure (9). As the liver is a membrane-covered organ, liver congestion can increase LS. Ultrasonography has recently been used to measure LS in order to evaluate congestive hepatopathy in HF patients. First, a vibration-controlled transient elastography (FibroScan®, Echosens, Paris, France), which was originally developed to evaluate liver fibrosis in patients with viral hepatitis, alcoholic lover disease, or primary biliary cirrhosis, is introduced to measure LS (*Figure 1*) (10,11). The median of 10 consecutive measurements was used as the LS for a given subject, and expressed in units of kilopascals (kPa). The normal range of LS is generally defined less than 7.0 kPa, and liver cirrhosis more than 12.5 kPa.

Previous studies show that LS is influenced by CVP (12,13). Millonig *et al.* (13) demonstrate that LS is a direct function of CVP by using pig models; they found that clamping the upper and lower vena cava, portal vein, and hepatic artery increases LS in a linear manner (R=1.0,

P<0.01). This suggests that LS might be a surrogate marker of liver congestion in HF patients. Accordingly, clinical studies revealed that LS is significantly elevated in patients with acute decompensated HF (*Figure 1*) (14,15). Taniguchi *et al.* (16) found that LS is strongly correlated with CVP estimated by pulmonary artery catheter in patients with HF (*Figure 2*). The accuracy, sensitivity, and specificity of LS ≥10.6 kPa to detect increased CVP >10 mmHg (normal range of CVP is ≤10 mmHg) were 0.90, 0.85, and 0.93, respectively. They conclude that LS may be an accurate noninvasive diagnostic method to assess CVP in patients with HF.

Besides a vibration-controlled transient elastography, shear wave elastography (SWE) can be used to assess LS on the basis of the propagation velocity of shear waves (*Figure 3*) (17). FibroScan® uses mechanical vibrations to generate shear waves, whereas SWE utilizes ultrasound as a source of shear waves and measures the horizontal propagation velocity of shear waves. Using an SWE method (i.e., Virtual Touch Quantification, VTQ®, Siemens, Erlangen, Germany), Yoshitani *et al.* (18) report that LS is
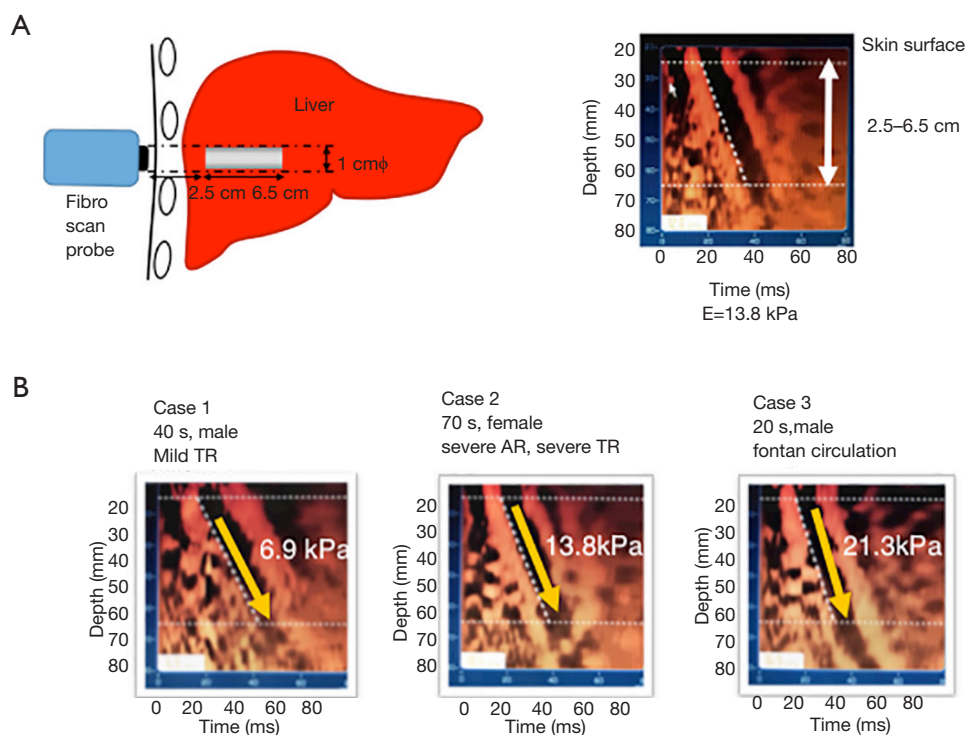
Figure 1 Liver stiffness by FibroScan®. (A) Panels show how to measure liver stiffness by FibroScan®. The operator selected a portion of the right liver lobe at least 6 cm thick, free of large vascular structures and gallbladder (left panel). The propagation of an elastic shear wave induced by low amplitude and frequency vibrations are clearly shown as an ultrasound figure (an oblique broken line in right panel). LS is measured as a propagation velocity between 2.5 and 6.5 cm depth from skin surface, which results are expressed in kilopascals (kPa). A LS measurement is obtained as an average of 10 consecutive measurements at the same place. In general, less than 7.0 kPa is normal, and greater than 12.5 is considered as cirrhosis in assessing liver fibrosis. (B) The panels show LS in representative cases with cardiac diseases. In patients with right-sided hear failure (cases 2 and 3), LS is increased as compared to patient without HF (case 1). In particular, case 3 of single ventricle with Fontan circulation has a markedly elevated LS, which suggests liver cirrhosis accompanied with liver congestion. AR, aortic regurgitation; TR, tricuspid regurgitation; LS, liver stiffness; HF, heart failure.

significantly correlated with CVP (R=0.578, P<0.001) and that changes of LS after medical treatment are correlated with changes of CVP (*Figure 4*). Thus, LS has another role as a feasible surrogate measure of liver congestions in HF patients owing to its strong dependence on CVP.

In the clinical setting, the elevation of cholestatic enzymes including total bilirubin, gamma-glutamyltransferase (GGT), and alkaline phosphatase (ALP) have been characterized in cardiac hepatopathy, which is relatively common in HF patients (19-21). Taniguchi *et al.* (16) reported that LS correlated with total bilirubin (R=0.56, P<0.001), GGT (R=0.45, P<0.001), and ALP (R=0.47, P<0.001), which may be supported by a previous study that found modest but significant correlations of the cholestatic enzymes with CVP (21). In addition, the

parameters of liver function are related to morbidity and mortality in HF patients (19,20), however, the prognostic information of liver function abnormalities in HF patients was blunted by elevated CVP (21). Namely, abnormal liver function tests in HF may be simply a result of a poor hemodynamic status.

In contrast, chronic liver congestion causes hepatic fibrosis and cirrhosis (*Figure 5*). Although the hepatic histological development in HF patients are complex (6,7), hepatic fibrosis is an important issue in the management of patients with advanced HF as liver fibrosis in patients with Fontan circulation is a critical issue (22). As there are no reliable biomarkers or hemodynamic parameters for the determination of liver fibrosis in patients with Fontan circulation, direct assessment of hepatic
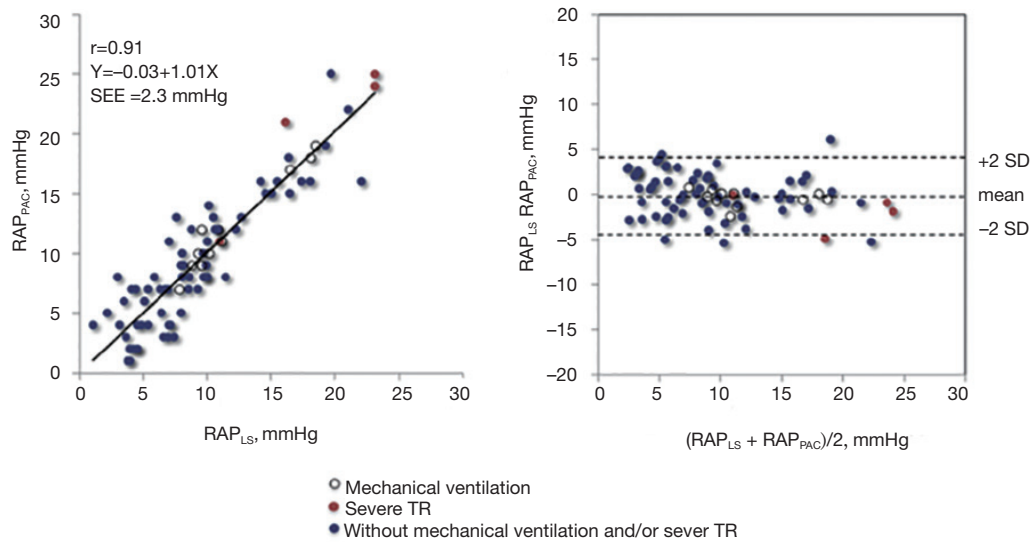
Figure 2 Close correlation between RAP by PAC and RAP by LS. Estimated RAP by LS is calculated by the following equation; RAP $= -5.9 + 6.8 \ln(LS)$. Quoted from reference (16). PAC, pulmonary artery catheter; RAP, right atrial pressure; LS, liver stiffness.
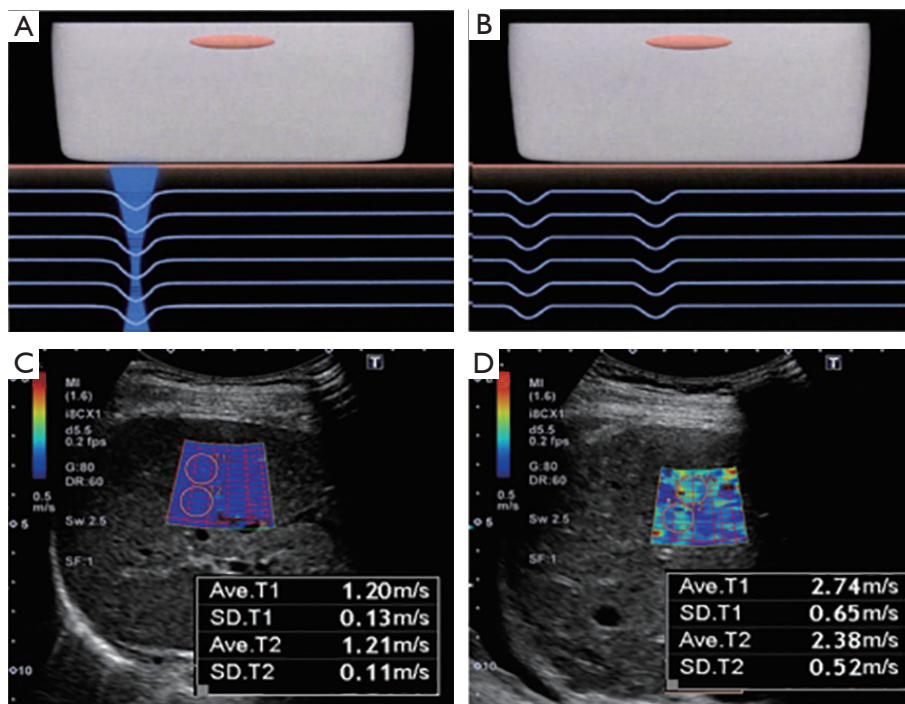

Figure 3 Liver stiffness by share wave elastography. (A) It shows tissue displacement by push pulse to generate share wave; (B) it illustrates their horizontal propagation. SWE can estimate LS from the horizontal propagation velocity of share wave. Unlike FibroScan®, LS is measured as a velocity (m/s); (C) a blue color region means propagation velocities of share waves in a healthy volunteer obtained from a commercial available system (Aplio i 900, Toshiba Medical Systems Corporation, Tochigi, Japan). An average propagation velocity (Ave. T1 or T2) and a standard deviation (SD. T1 or T2) in each region of interest (orange circle) are shown as normal values; (D) in contrast, a mosaic pattern region is obtained from a patient with Fontan circulation. As compared to a healthy volunteer, a higher propagation velocity (Ave. T1 or T2) in each region of interest (orange circle) was observed, and means elevated LS. LS, liver stiffness.
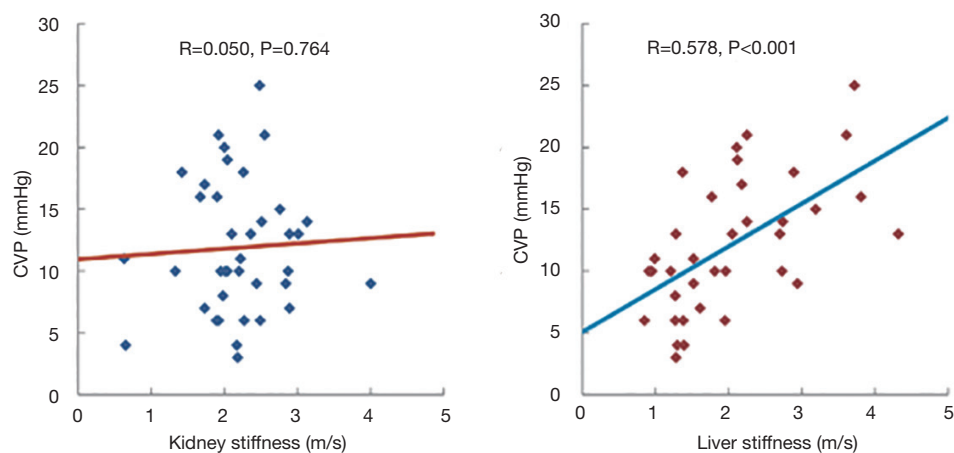
cdt.amegroups.com   *Cardiovasc Diagn Ther* 2018;8(1):57-69

Figure 4 Correlation between organ stiffness and central venous pressure. CVP significantly correlates with liver stiffness by VTQ®, however, not with kidney stiffness. Quoted from reference (18). CVP, central venous pressure.
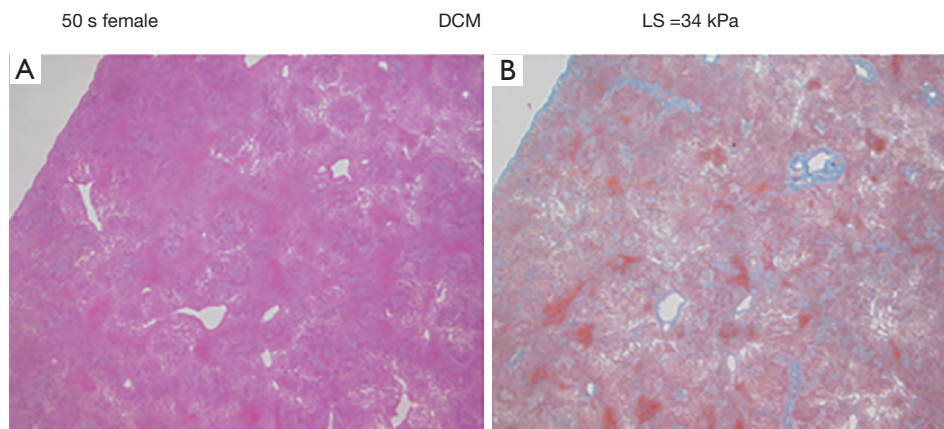

Figure 5 Liver fibrosis accompanied with liver congestion. Panels show the autopsy findings of liver in patients with dilated cardiomyopathy. The FibroScan® study performed at 3 months before autopsy showed markedly elevated LS (34 kPa). In addition to severe congestion (A: hematoxylin stain), diffuse fibrosis, in particular centrilobular regions is observed (B: Masson trichrome stain).

architecture might still be the most reliable evaluation method (22). Despite a lack of data supported by liver biopsy, preliminary studies on transient elastography (23-25) show that LS is significantly associated with clinical liver cirrhosis diagnosed on the basis of blood tests, ultrasound, and gastric endoscopy findings in patients with Fontan circulation. In addition, the clinical implications of LS have been studied in patients with severe HF who have undergone left ventricular assist device (LVAD) implantation (26,27). As in studies of patients with HF, CVP is reported to be the major determinant of LS in the end-stage HF patients with LVAD. Potthoff *et al.* (26) reported the strong correlation of preoperative LS with preoperative CVP (r=0.793, P<0.001), and a moderate correlation (R=0.511, P<0.01) was reported by Nishi *et al.* (27). Both studies showed LS decreases significantly after LVAD implantation, however, LS gradually decreased during the postoperative period in particular in patients with higher preoperative LS >7.0 kPa (27), and more evident changes, but not to normal values, were observed more than 1 year after LVAD implantations (26). The sequential changes suggest that intrinsic liver damage including fibrosis may be associated with LS even after LVAD implantation as liver fibrosis also is a significant determinant of LS in patients with LVAD (26). In addition, these studies indicate that preoperative LS is associated with
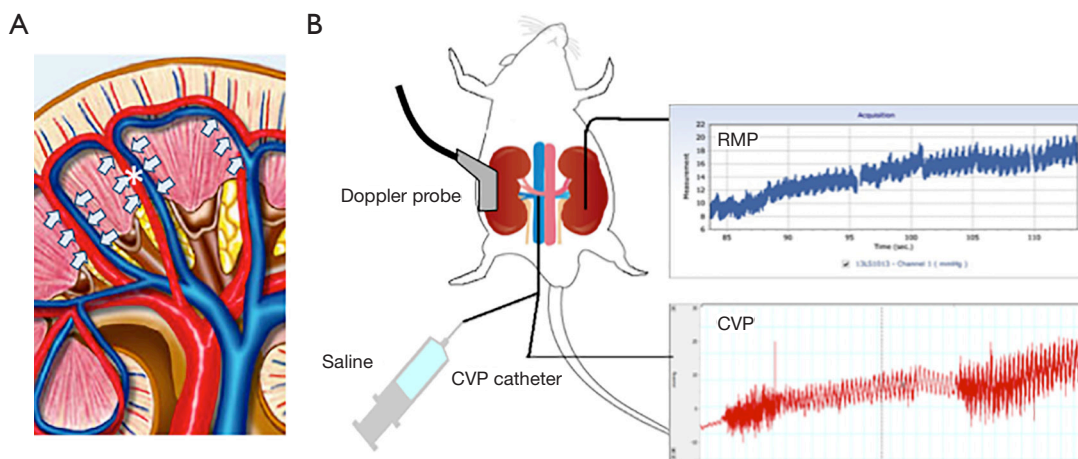
Figure 6 Conceptual scheme of renal congestion and the rat model. (A) The panel shows a hypothetical image of compressed interlobar vessels (*) in the renal parenchymal regions accompanied with increased parenchymal pressure; (B) the panel shows conceptual scheme of an acute renal congestion rat model. A 5 mL of saline was injected via a central venous in 30 seconds until a 15 mmHg of CVP. Right parts in (B) show time-pressure relations of RMP and CVP obtained from simultaneous recording. CVP, central venous pressure; RMP, renal medulla pressure.

clinical outcomes after LVAD implantation; LS is higher in the non-surviving population (26,27) and in patients who required a right ventricular assist device (RVAD) (27). Although these studies are preliminary, LS may have an additional value to predict clinical outcomes more than cholestatic enzymes.

In summary, LS measured by ultrasonography is mainly determined by CVP. Therefore, LS may be a reliable, noninvasive indicator of congestive hepatopathy. Furthermore, LS is expected to be a noninvasive surrogate marker of liver fibrosis and cirrhosis in patients with advanced right-sided HF including Fontan circulation and terminal HF patients who require LVAD or transplantation. Based on the association not only with liver congestion but also with pathological changes, LS might be a more useful prognostic marker more than serum liver function tests HF patients, although this requires further evaluation.

There are some limitations to use LS in assessing HF patients. First, the relations of LS with pathological findings should be revealed. The dependence on congestion has been demonstrated, however, the associations with liver damage including fibrosis and necrosis due to HF have to be resolved if LS derived HF managements are performed.

Secondary, previous studies did not show the prognostic impact of LS in HF patients.

In future, large scale studies could be carried out to resolve the agenda, which will be enable since this technique

has an acceptable reproducibility.

Renal congestion

Cardiorenal syndrome is widely recognized as an important pathophysiological mechanism of HF, because reduced renal function is associated with adverse clinical outcomes in patients with HF (28-30). Although there are various mechanisms of cardiorenal syndrome, the importance of renal congestion has become recognized (31,32). The presence of renal congestion in HF is currently estimated on the basis of increased CVP. As the kidneys are encapsulated organs like the liver, renal stiffness might increase as a result of congestion. However, a previous study failed to find a significant correlation between renal stiffness and CVP (*Figure 4*) (18).

We recently reported the usefulness of Doppler-derived intrarenal venous flow (IRVF) pattern for the assessment of renal congestion in patients with HF (33). Despite a lack of studies regarding the role of ultrasound in assessing renal congestion, we would like to introduce the rationale and clinical implications of our method. Renal congestion mainly occurs in renal parenchymal regions accompanied by increased renal interstitial pressure (34). The altered parenchymal conditions may directly compress vessels in the renal parenchymal regions, which reduce vessel capacitance or compliance accompanied by increased CVP (*Figure 6*). The changes to vessel morphology and function

cdt.amegroups.com

CVP 2 mmHg
IRP 4 mmHg
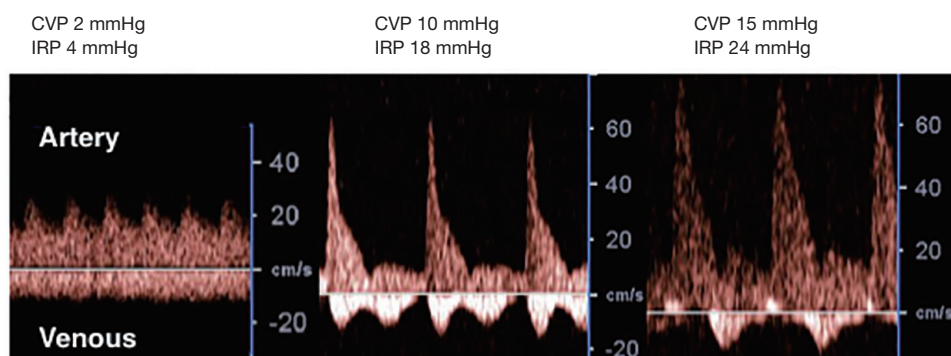
CVP 10 mmHg
IRP 18 mmHg

CVP 15 mmHg
IRP 24 mmHg

Figure 7 Changes of intrarenal Doppler flow by acute renal congestion. Sequential images of intrarenal Doppler flow at baseline, a 10 mmHg of CVP, and a 15 mmHg of CVP. Note IRP is relatively high compared to CVP. CVP, central venous pressure; IRP, intra-renal medulla pressure.

consequently affect vessel flow. We use intrarenal Doppler ultrasound (IRD) to evaluate intrarenal hemodynamics. We evaluate changes of Doppler signals at interlobar vessels because they are adjacent to renal parenchymal regions (*Figure 6*).

As part of a preliminary experimental study (*Figure 6*), we examined the changes of Doppler signals at the interlobar vessels in a rat model of acute congestion (*Figure 7*). To create an acute renal congestion model, we used Wistar rats (n=12, 16–18 weeks, 371.5±9.9 g), and injected 5 mL saline intravenously over 30 seconds, which was repeated until the CVP increased to 10 or 15 mmHg (*Figure 6*). We confirmed the increase of renal medulla pressure (RMP) accompanied by increased CVP by using a catheter with a fiber-optic pressure sensor (FISO-LS-PT9, FISO Technologies, Quebec, Canada) (*Figure 6*). CVP at baseline was 2.5±1.2 mmHg, and RMP at baseline was 6.1±1.8 mmHg. RMP at CVP of 10 mmHg was ranged from 12 to 26 mmHg (16.9±2.7 mmHg) and RMP at CVP of 15 mmHg was ranged from 15 to 30 mmHg (20.7±1.8 mmHg). Compared to baseline, the velocity of the renal interlobar artery increased dramatically, with rapid deceleration and increased renal medulla pressure (*Figure 7*). Resistance index (RI) of interlobar artery, which was calculated as (maximum velocity-minimum velocity)/maximum velocity, was significantly increased accompanied with increasing of CVP and RDP; RI at baseline was 0.45±0.05, RI at CVP of 10 mmHg was 0.66±0.11, and RI at CVP of 15 mmHg was 0.8±0.14 (P<0.001 ANOVA). In contrast, venous flow patterns are marked by the appearance

of discontinuous flow with increased RMP. As the RMP increases, the flow changes from biphasic to monophasic. The venous flow at baseline showed only continuous pattern. The flow pattern at CVP of 10 mmHg was altered to biphasic (n=10) and monophasic (n=2). At CVP of 15 mmHg, almost rats showed monophasic pattern (n=11). These alterations suggest that changes of vessel compliance and capacitance due to renal congestion induce increased RMP. Thus, intrarenal Doppler profile is a surrogate marker of renal congestion.

In clinical settings, IRD studies can be performed using a commercially available Vivid E9 echocardiography system (GE Healthcare, Horton, Norway). In addition, a variable-frequency 2.5–5-MHz sector transducer can be adapted, yielding data similar to those obtained from a convex array probe. IRD is usually recorded in the right kidney, with the patient in the left lateral decubitus position. We have already confirmed that the data do not differ from those obtained in the right kidney independent of patient position. The velocity range of the color Doppler is set to approximately 12–16 cm/s in order to determine interlobar vessels, and the sample volume is set on the basis of the color Doppler signals derived from the interlobar vessels (*Figure 8*).

Furthermore, patients with HF can also exhibit intrarenal Doppler profiles similar to those seen in an acute renal congestion model (*Figure 8*). The major determinant of the IRD profile is CVP and not cardiac index (*Figure 9*) (32). Although the majority of patients with a monophasic pattern have elevated CVP >10 mmHg,
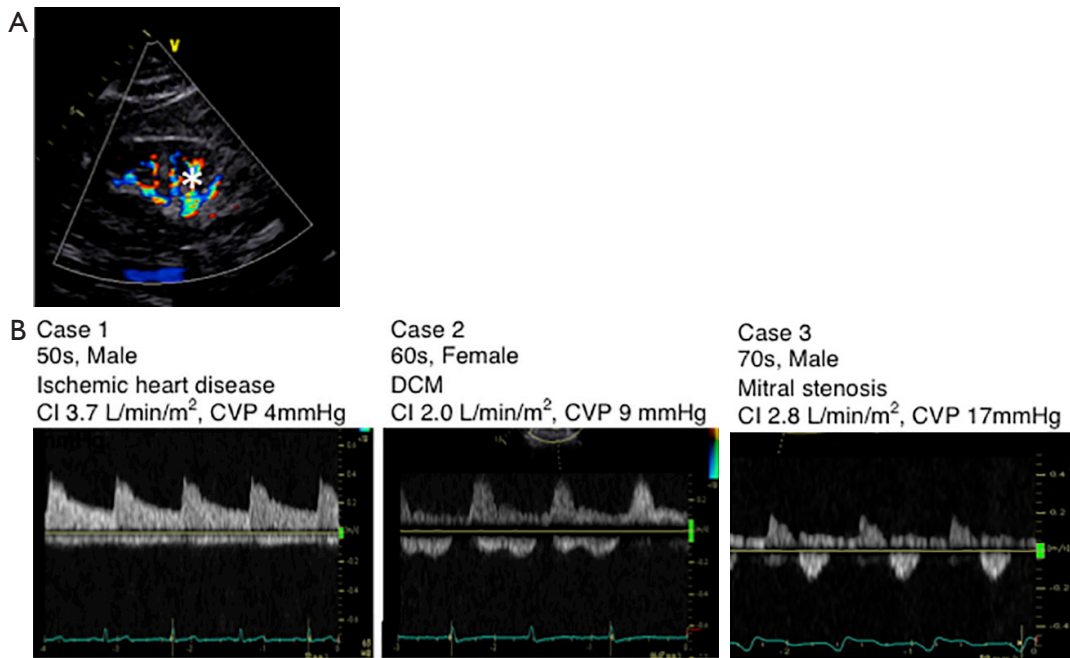
Figure 8 Intra-renal color Doppler image and IRVF pattern. (A) Intra-renal color Doppler image in a normal subject. A Doppler sample point at interlobar vessels is marked with an asterisk; (B) representative cases of each IRVF pattern. Case 1 is a continuous IRVF with normal hemodynamic profile. Case 2 with DCM showed a biphasic discontinuous IRVF pattern with slightly increased CVP and reduced CI. Case 3 with mitral stenosis and right-sided heart failure had a monophasic discontinuous IRVF pattern with significantly increased CVP and preserved CI. IRVF, intrarenal venous flow; CVP, central venous pressure; CI, cardiac index.
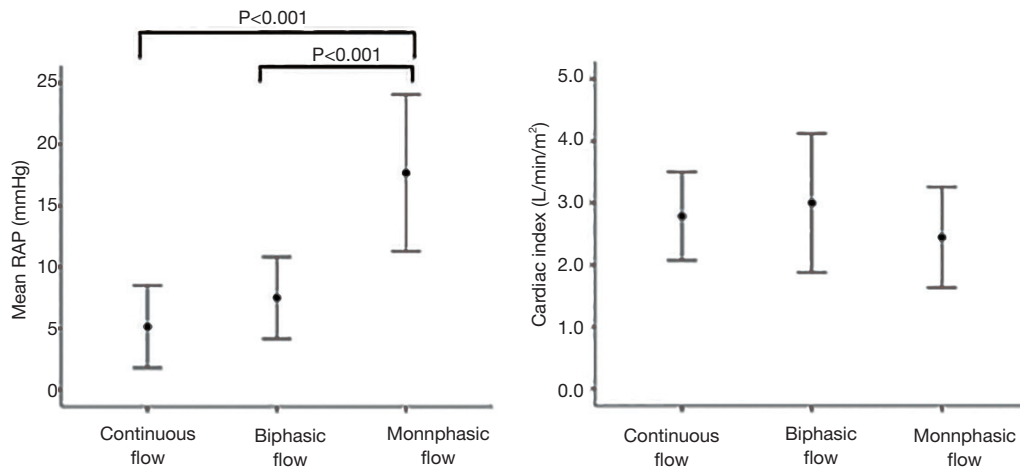

Figure 9 Comparisons of between IRVF patterns. In our cohort of first heart failure hospitalization, RAP from pulmonary artery catheter studies at stable condition after medications is shown in left panel. Mean RAP in patients with monophasic flow is significantly higher than other flow pattern. Mean RAP in patients with biphasic flow is slightly higher, but not significant compared to patients with continuous flow. As shown in right panel, cardiac index did not differ between IRVF patterns. IRVF, intrarenal venous flow; RAP, right atrial pressure.
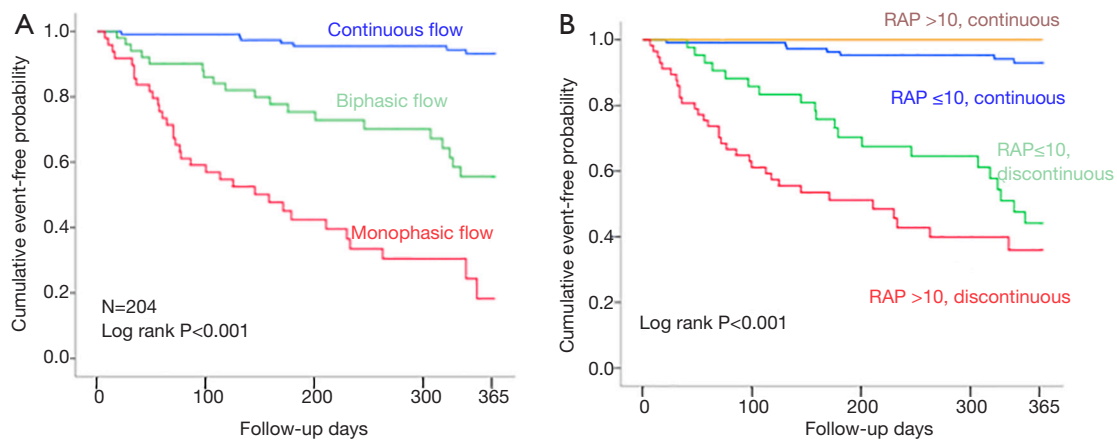
cdt.amegroups.com *Cardiovasc Diagn Ther* 2018;8(1):57-69

Figure 10 Comparisons of clinical outcomes according to IRVF. (A) Kaplan-Meier curves at 1-year follow-up for the probability of freedom from death from cardiac causes and unplanned hospitalizations for heart failure of three classifications of IRVF; (B) Kaplan-Meier curves of four classifications based on the IRVF continuous and discontinuous patterns and right atrial pressure (RAP). Independent of RAP estimated by echocardiography, IRVF could distinguish high risk heart failure patients. Quoted from reference (32). IRVF, intrarenal venous flow; RAP, right atrial pressure.

patients with a biphasic pattern have modestly elevated CVP. In the comparisons with the prevalence of right atrial pressure estimation based on inferior vena cava observation (eRAP) >10 mmHg, elevated eRAP >10 mmHg is observed in 94% of HF patients with a monophasic pattern, 60.8% in HF patients with a biphasic pattern, and 13.7% in in HF patients with a continuous pattern, respectively. These findings suggest that a continuous pattern is observed in the setting of normal CVP, and a monophasic pattern strongly associates with elevated CVP. However, a biphasic pattern could not be determined based on the CVP level.

As the main clinical implication of the IRD profile, IRVF pattern is an independent determinant of primary endpoints defined as death from cardiovascular disease or unplanned hospitalization for HF (*Figure 10*). Univariate and multivariable Cox proportional hazard model analyses were summarized in *Table 2*. As shown in the multivariable model, biphasic and monophasic flow pattern, but not CVP >10 mmHg, were identified as a significant predictor of the endpoints independently of sodium and BNP levels. In particular, its significance as a prognostic marker has been confirmed to be independent of eRAP (*Figure 10*). The results mean that a biphasic pattern, which does not depend on CVP as above

mentioned, may be more sensitive for renal congestion as compared to eRAP.

In addition, we strongly expect that IRD-guided therapy can achieve optimal decongestion. As mentioned earlier, the IRD profile may be superior to eRAP for the estimation of clinical outcomes, which suggests that IRD may be a more reliable surrogate of renal congestion than CVP. A representative case supporting our concept is presented in *Figure 11*. Nevertheless, large-scale prospective studies are required to corroborate our concept.

In almost all cases, pulsed Doppler waveforms of the interlobar arteries and veins are recorded. Particular care should be taken to ensure the patient holds their breath during IRD recording. Because the region of interest is small, it may be moved out of view if the patient cannot hold their breath. Therefore, this technique may be unsuitable during the acute phase of HF exacerbation. In addition, the ability of IRD to predict clinical outcome in HF must be assessed in large-scale, multicenter studies. The present study could not determine which factor is more important in determining the IRVF profile, why a discrepancy is present between the CVP level and renal congestion, and how concomitant factors including diabetes and hypertension contribute to renal parenchymal

66

Seo et al. Assessment of organ congestion by ultrasonography

Table 2 Univariate and multivariable predictors of death from cardiac causes or unplanned hospitalization for heart failure by the cox proportional hazard model

Predictor	Univariate		Multivariable model	
	HR (95% CI)	P value	HR (95% CI)	P value
Hemoglobin	0.79 (0.70–0.88)	<0.001		
BUN (per 10 mg/dL increase)	1.31 (1.14–1.50)	<0.001		
eGFR (per 10 increase)	0.98 (0.97–0.99)	0.006		
Sodium (per 1 mEq/L increase)	0.84 (0.74–0.91)	<0.001	0.93 (0.86–0.99)	0.02
BNP (per 100 pg/mL increase)	1.06 (1.04–1.08)	<0.001	1.05 (1.02–1.07)	<0.001
Loop diuretics	2.39 (1.38–4.16)	0.002		
LVEF (per 10% increase)	0.85 (0.76–0.94)	0.002		
E/E' >15	2.77 (1.66–4.64)	<0.001		
LAVI (per 10-mL increase)	1.19 (1.09–1.30)	<0.001		
RV-FAC (per 10% increase)	0.67 (0.55–0.79)	<0.001		
Moderate or severe TR	2.81 (1.60–4.93)	<0.001		
RAP >10 mmHg	5.26 (2.93–9.43)	<0.001		
RI ≥0.70	1.78 (1.06–3.00)	0.03		
HV-S/D <0.55 (lower quartile)	3.99 (2.38–6.69)	<0.001		
IRVF pattern				
Continuous	1	–		
Biphasic	8.23 (3.45–19.7)	<0.001	6.85 (2.82–16.6)	<0.001
Monophasic	23.1 (10.0–53.5)	<0.001	17.8 (7.62–41.9)	<0.001

Quoted from reference (33). HR, hazard ratio; CI, confidence interval; BNP, brain natriuretic peptide; BUN, blood urea nitrogen; eGFR, estimated glomerular filtration rate; E/E', ratio of early diastolic peak velocity of Doppler transmitral flow to early diastolic mitral annular velocity; HV-S/D, ratio of hepatic vein systolic to diastolic flow velocities; IRVF, intrarenal venous flow; LVEF, left ventricular ejection fraction; RAP, right atrial pressure; RI, resistance index; RV-FAC, right ventricular fractional area change ratio.

compliance. Therefore, future studies are needed to clarify the related pathophysiology.

Conclusions

Decongestion is key in the management of HF patients.

In clinical settings, objective methods to evaluate organ congestion, in particular liver and kidney congestion, using ultrasonography may be useful for assessing decongestion status in patients with HF. As there is currently no established method at present, further studies are required to determine a feasible marker for determining optimal
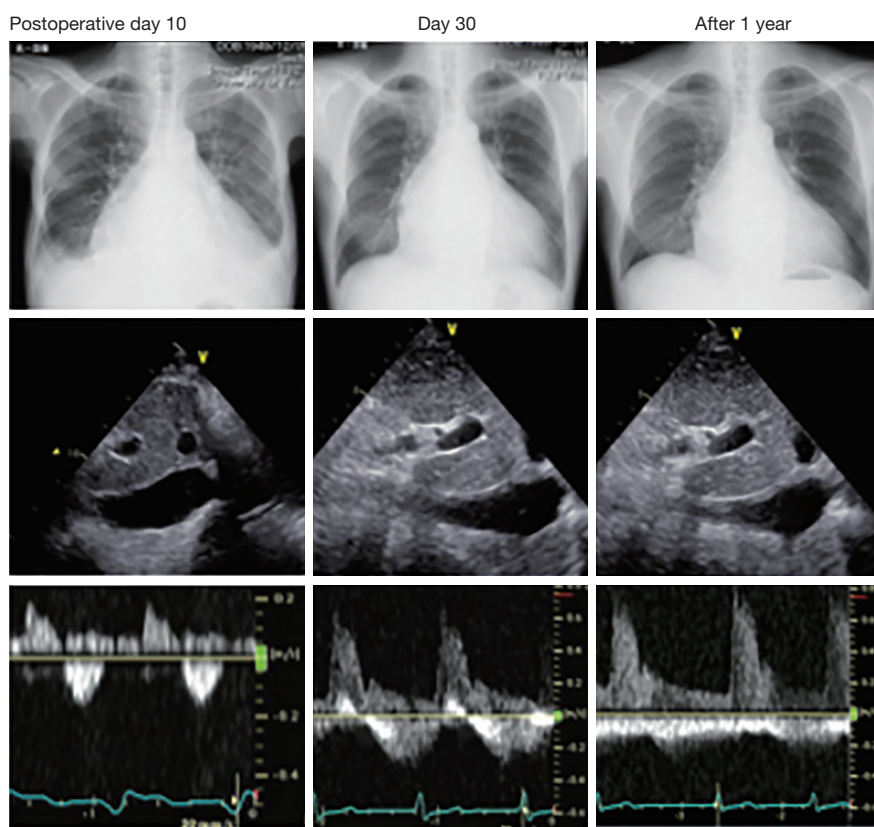
Figure 11 Changes of chest X-ray, inferior vena cava, IRVF by IRD guided therapy in a case of post MVR, and TAP. This 70s male patient (same case in *Figure 8*, case 3) showed residual congestion at postoperative day 10. Bilateral pleural effusion, distended IVC without respiratory variation, and monophasic IRVF. After aggressive decongestion therapy using ultrafiltration and use of tolvaptan, which is a drug for SIADH however, is available as a diuretic in Japan, pleural effusion was disappeared, and IVC was distended yet, but respiratory variation of IVC was observed at postoperative day 30. Based on the chest X-ray and IVC findings, it was considered that optimal decongestion was achieved. However, IRVF still showed a discontinuous pattern. Therefore, physicians continued administration of tolvaptan with furosemide, because it was considered that the patient might be still at vulnerable heart failure condition with residual renal congestion based on clinical outcome shown in *Figure 10*. After spending a year, the patient was carefully observed at our outpatient clinic, and continuous IRVF pattern could be observed. Currently, he is stable and has not never been rehospitalized. IRVF, intrarenal venous flow; IRD, intrarenal Doppler ultrasound; MVR, mitral valve replacement; TAP, tricuspid annuloplasty; IVC, inferior vena cava; SIADH, syndrome of inappropriate secretion of antidiuretic hormone.

decongestion.

Footnote

Conflicts of Interest: The authors have no conflicts of interest to declare.

References

1. Go AS, Mozaffarian D, Roger VL, et al. Heart disease and stroke statistics--2014 update: a report from the American Heart Association. Circulation 2014;129:e28-292.
2. Heidenreich PA, Albert NM, Allen LA, et al. Forecasting the impact of heart failure in the United States: a policy statement from the American Heart Association. Circ Heart Fail 2013;6:606-19.
3. Jencks SF, Williams MV, Coleman EA. Rehospitalizations among patients in the Medicare fee-for-service program.

68

Seo et al. Assessment of organ congestion by ultrasonography

N Engl J Med 2009;360:1418-28.

4. Wang CS, FitzGerald JM, Schulzer M, et al. Does this dyspneic patient in the emergency department have congestive heart failure? JAMA 2005;294:1944-56.

5. Gheorghiade M, Follath F, Ponikowski P, et al. Assessing and grading congestion in acute heart failure: a scientific statement from the acute heart failure committee of the heart failure association of the European Society of Cardiology and endorsed by the European Society of Intensive Care Medicine. Eur J Heart Fail 2010;12:423-33.

6. Nagueh SF, Smiseth OA, Appleton CP, et al. Recommendations for the Evaluation of Left Ventricular Diastolic Function by Echocardiography: An Update from the American Society of Echocardiography and the European Association of Cardiovascular Imaging. J Am Soc Echocardiogr 2016;29:277-314.

7. Myers RP, Cerini R, Sayegh R, et al. Cardiac hepatopathy: clinical, hemodynamic, and histologic characteristics and correlations. Hepatology 2003;37:393-400.

8. Sherlock S. The liver in heart failure; relation of anatomical, functional, and circulatory changes. Br heart J 1951;13:273-93.

9. Megalla S, Holtzman D, Aronow WS, et al. Predictors of cardiac hepatopathy in patients with right heart failure. Med Sci Monit 2011;17:CR537-41.

10. Sandrin L, Fourquet B, Hasquenoph JM, et al. Transient elastography: a new noninvasive method for assessment of hepatic fibrosis. Ultrasound Med Biol 2003;29:1705-13.

11. Friedrich-Rust M, Ong MF, Martens S, et al. Performance of transient elastography for the staging of liver fibrosis: a meta-analysis. Gastroenterology 2008;134:960-74.

12. Lebray P, Varnous S, Charlotte F, et al. Liver stiffness is an unreliable marker of liver fibrosis in patients with cardiac insufficiency. Hepatology 2008;48:2089.

13. Millonig G, Friedrich S, Adolf S, et al. Liver stiffness is directly influenced by central venous pressure. J Hepatol 2010;52:206-10.

14. Hopper I, Kemp W, Porapakkham P, et al. Impact of heart failure and changes to volume status on liver stiffness: non-invasive assessment using transient elastography. Eur J Heart Fail 2012;14:621-7.

15. Colli A, Pozzoni P, Berzuini A, et al. Decompensated chronic heart failure: increased liver stiffness measured by means of transient elastography. Radiology 2010;257:872-8.

16. Taniguchi T, Sakata Y, Ohtani T, et al. Usefulness of transient elastography for noninvasive and reliable estimation of right-sided filling pressure in heart failure.

Am J Cardiol 2014;113:552-8.

17. Dahl JJ, Palmeri ML, Nightingale KR, et al. Shear wave velocity estimation using acoustic radiation force impulsive excitation in liver in vivo. In: IEEE Ultrasonics Symposium, 2006. Vancouver: IEEE, 2006;1156-60.

18. Yoshitani T, Asakawa N, Sakakibara M, et al. Value of Virtual Touch Quantification elastography for assessing liver congestion in patients with heart failure. Circ J 2016;80:1187-95.

19. Allen LA, Felker GM, Pocock S, et al. Liver function abnormalities and outcome in patients with chronic heart failure: data from the Candesartan in Heart Failure: Assessment of Reduction in Mortality and Morbidity (CHARM) program. Eur J Heart Fail 2009;11:170-7.

20. Poelzl G, Ess M, Mussner-Seeber C, et al. Liver dysfunction in chronic heart failure: Prevalence, characteristics and prognostic significance. Eur J Clin Invest 2012;42:153-63.

21. van Deursen VM, Damman K, Hillege HL, et al. Abnormal liver function in relation to hemodynamic profile in heart failure patients. J Card Fail 2010;16:84-90.

22. Goldberg DJ, Surrey LF, Glatz AC, et al. Hepatic Fibrosis Is Universal Following Fontan Operation, and Severity is Associated With Time From Surgery: A Liver Biopsy and Hemodynamic Study. J Am Heart Assoc 2017;6. pii:e004809.

23. Friedrich-Rust M, Koch C, Rentzsch A, et al. Noninvasive assessment of liver fibrosis in patients with Fontan circulation using transient elastography and biochemical fibrosis markers. J Thorac Cardiovasc Surg 2008;135:560-7.

24. Yoo BW, Choi JY, Eun LY, et al. Congestive hepatopathy after Fontan operation and related factors assessed by transient elastography. J Thorac Cardiovasc Surg 2014;148:1498-505.

25. Wu FM, Opotowsky AR, Raza R, et al. Transient elastography may identify Fontan patients with unfavorable hemodynamics and advanced hepatic fibrosis. Congenit Heart Dis 2014;9:438-47.

26. Potthoff A, Schettler A, Attia D, et al. Liver stiffness measurements and short-term survival after left ventricular assist device implantation: A pilot study. J Heart Lung Transplant 2015;34:1586-94.

27. Nishi H, Toda K, Miyagawa S, et al. Novel method of evaluating liver stiffness using transient elastography to evaluate perioperative status in severe heart failure. Circ J 2015;79:391-7.

28. Smith GL, Lichtman JH, Bracken MB, et al. Renal

impairment and outcomes in heart failure: systematic review and meta-analysis. J Am Coll Cardiol 2006;47:1987-96.

29. Damman K, Navis G, Voors AA, et al. Worsening renal function and prognosis in heart failure: systematic review and meta-analysis. J Card Fail 2007;13:599-608.

30. Butler J, Chirovsky D, Phatak H, et al. Renal function, health outcomes, and resource utilization in acute heart failure: a systematic review. Circ Heart Fail 2010;3:726-45.

31. Damman K, van Deursen VM, Navis G, et al. Increased central venous pressure is associated with impaired renal function and mortality in a broad spectrum of patients with cardiovascular disease. J Am Coll Cardiol 2009;53:582-8.

32. Mullens W, Abrahams Z, Francis GS, et al. Importance of venous congestion for worsening of renal function in advanced decompensated heart failure. J Am Coll Cardiol 2009;53:589-96.

33. Iida N, Seo Y, Sai S, et al. Clinical implications of intrarenal hemodynamic evaluation by Doppler ultrasonography in heart failure. JACC Heart Fail 2016;4:674-82.

34. Burnett JC Jr, Knox FG. Renal interstitial pressure and sodium excretion during renal vein constriction. Am J Physiol 1980;238:F279-82.